INTERNATIONAL JOURNAL FOR NUMERICAL METHODS IN FLUIDS
Int. J. Numer. Meth. Fluids 2002; **38**:1–19 (DOI: 10.1002/fld.201)

A finite volume solver for 1D shallow-water equations applied to an actual river

N. Goutal*,† and F. Maurel

EDF—Laboratoire National d'Hydraulique, 6, Quai Watier, 78400 Chatou, France

SUMMARY

This paper describes the numerical solution of the 1D shallow-water equations by a finite volume scheme based on the Roe solver. In the first part, the 1D shallow-water equations are presented. These equations model the free-surface flows in a river. This set of equations is widely used for applications: dam-break waves, reservoir emptying, flooding, etc. The main feature of these equations is the presence of a non-conservative term in the momentum equation in the case of an actual river. In order to apply schemes well adapted to conservative equations, this term is split in two terms: a conservative one which is kept on the left-hand side of the equation of momentum and the non-conservative part is introduced as a source term on the right-hand side. In the second section, we describe the scheme based on a Roe Solver for the homogeneous problem. Next, the numerical treatment of the source term which is the essential point of the numerical modelisation is described. The source term is split in two components: one is upwinded and the other is treated according to a centred discretization. By using this method for the discretization of the source term, one gets the right behaviour for steady flow. Finally, in the last part, the problem of validation is tackled. Most of the numerical tests have been defined for a working group about dam-break wave simulation. A real dam-break wave simulation will be shown. Copyright © 2002 John Wiley & Sons, Ltd.

KEY WORDS: shallow-water equations; river; source terms; finite volume; Roe scheme

1. INTRODUCTION

In this paper, we focus on the resolution of the 1D shallow-water equations. These equations model the free-surface flow in rivers. They are deduced from the conservation of mass and momentum for an incompressible free-surface fluid under the assumptions of hydrostatic pressure and uniform distribution of the velocity along the vertical axis.

This set of equations is used for a large range of applications related to free-surface flows, as for instance: dam-break wave, reservoir emptying, flooding, etc. These applications present different features:

- very fast unsteady flow with dry areas for the dam-break wave simulation;

*Correspondence to: N. Goutal, EDF—Laboratoire National d'Hydraulique, 6, Quai Watier, 78400 Chatou, France.
†E-mail: nicole.goutal@edf.fr

Received 2 September 1999
Revised 27 January 2001

- quasi-steady flow in case of reservoir emptying with occurrence of dry areas;
- steady flow in rivers.

The purpose of this work is to build numerical methods designed to handle the above-mentioned features. We present here a resolution of the 1D shallow-water equations in the case of an actual river by a finite volume scheme based on the Roe solver.

In the case of a rectangular channel with a flat bottom, the shallow-water equations are equivalent to the homogeneous isentropic Euler equations. Therefore, it is natural to apply standard methods developed for these equations. We have chosen a finite volume scheme based on a Roe Solver because this scheme is widely used [1–8] and has shown its robustness in various applications.

However, in the case of an actual river, because of the slope of the bottom and the variation of the river width, the pressure term becomes a non-conservative term. Up to now, little work has been devoted to the numerical treatment of the source term in the case of an actual river. In order to apply the scheme adapted to the case of a rectangular channel, this non-conservative term has been split in two terms: the first one is written in a conservative form on the left-hand side (LHS), the second one leads to a source term on the right-hand side (RHS). It is necessary to solve difficult source terms for this method. In particular, one of the main difficulties to achieve is that a flow 'at rest' stays 'at rest' without any perturbation in case of complex geometry.

This paper is organised as follows. In the first section we introduce the set of equations chosen to model free-surface flow in a river and we give its main features. In the second section we describe the scheme used for the homogeneous problem. In the third section we deal with the numerical treatment of the source terms. Finally, in the fourth section the problem of validation is tackled. Some numerical results obtained with the code MASCARET are given. Most of the numerical tests have been defined for a European working group about dam-break wave simulation (Concerted Action on Dam-Break Modeling (CADAM)).

2. THE 1D SHALLOW-WATER EQUATIONS

The 1D free-surface flows in rivers (see Figure 1) are governed by the shallow-water equations. They result from a vertical integration of the Navier–Stokes equations under the assumption that the fluid is incompressible and the pressure hydrostatic.

The set of equations is in terms of discharge $Q(x,t)$ and hydraulic section $S(x,t)$:

$$\begin{cases} \dfrac{\partial S}{\partial t} + \dfrac{\partial Q}{\partial x} = 0 & (1) \\ \dfrac{\partial Q}{\partial t} + \dfrac{\partial}{\partial x}\left(\dfrac{Q^2}{S}\right) + gS\dfrac{\partial Z}{\partial x} = -gSJ & (2) \end{cases}$$

where $Z(x,t)$ is the free-surface level, $S(x,t)$ is the hydraulic section, $Q(x,t)$ is the discharge, g is the gravity, J the friction head loss given by $J = (Q^2)/(K^2 S^2 R_h^{4/3})$, R_h is the hydraulic radius and K the Strickler friction coefficient.

In case of a rectangular channel with a constant width and a flat bottom, the set of Equations (1) and (2) is equivalent to the isentropic Euler equations. The non-conservative

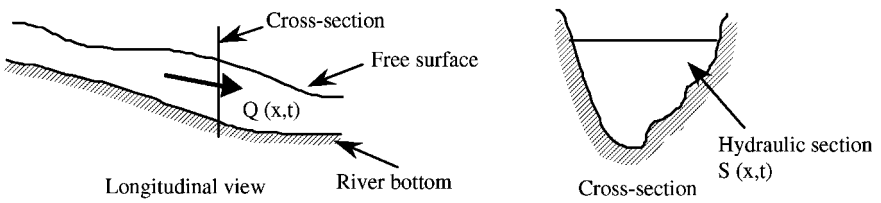

Figure 1. Schematic diagram of river, illustrating discharge $Q(x,t)$ and hydraulic section $S(x,t)$.

term $gS((\partial Z)/(\partial x))$ can be expressed as a conservative one $gh((\partial h)/(\partial x))$ (in this particular case $S = Lh(x,t)$ where $h(x,t)$ is the water depth), so that all the classical finite volume schemes developed for the Euler equations can be used.

However, for actual applications, the previous assumptions are no more valid and we have to deal with a non-conservative term $gS((\partial Z)/(\partial x))$ which is the integrated source. For this, two paths can be followed:

- The first one is to split this term in two parts. The conservative part equivalent to a pressure term, is written on the LHS; accordingly classical finite volume techniques can be applied and the non-conservative part (terms due to the bottom slope and to the variation of the channel width) is introduced on the RHS as a source term. Therefore, this splitting is based upon numerical instead of physical consideration.
- The second one is to keep this non-conservative term $gS((\partial Z)/(\partial x))$ on the LHS in order to keep a physical picture of the problem. Therefore, dealing with the term $gS((\partial Z)/(\partial x))$ necessitates the development of an adapted scheme in the framework of finite volume discretization [9–14].

We have chosen the first method because it allows one to use the same scheme as the one used for the shallow-water equations in the case of rectangular channels. The main drawback of this method is having to deal with source terms (terms due to the bottom slope and to the variation of the channel width) that are not physical. Consequently, the modelisation of these source terms must be performed in such a way that no artificial energy due to the bottom slope and to the variation of the channel width appears.

The term $gS((\partial Z)/(\partial x))$ can be rewritten by introducing a pressure term $P(x,S) = g\int_0^y S(x,z)\mathrm{d}z$, where y is the water depth equal to $y = Z - Z_\mathrm{f}$, Z_f being the bottom level.

In fact,

$$\frac{\partial P(x,S)}{\partial x} = gS\frac{\partial Z}{\partial x} + g\int_0^y \left(\frac{\partial S(x,z)}{\partial x}\right)_z \mathrm{d}z - gS\frac{\partial Z_\mathrm{f}}{\partial x} \tag{3}$$

Equations (1) and (2) can be rewritten by introducing Equation (3):

$$\begin{cases} \dfrac{\partial S}{\partial t} + \dfrac{\partial Q}{\partial x} = 0 & (4) \\ \dfrac{\partial Q}{\partial t} + \dfrac{\partial}{\partial x}\left(\dfrac{Q^2}{S} + P(x,S)\right) = g\displaystyle\int_0^y \left(\frac{\partial S(x,z)}{\partial x}\right)_z \mathrm{d}z - gS\frac{\mathrm{d}Z_\mathrm{f}}{\mathrm{d}x} - gSJ & (5) \end{cases}$$

The system defined by Equations (4) and (5) now reads:

$$\frac{\partial W(x,t)}{\partial t} + \frac{\partial F(x,W)}{\partial x} = G(x,W) \tag{6}$$

with

$$W = \begin{pmatrix} S \\ Q \end{pmatrix} \quad F(x,W) = \begin{pmatrix} Q \\ \dfrac{Q^2}{S} + P(x,S) \end{pmatrix}$$

$$G(x,W) = \begin{pmatrix} 0 \\ g\displaystyle\int_0^y \left(\frac{\partial S(x,z)}{\partial x}\right)_z \mathrm{d}z - gS\frac{\mathrm{d}Z_\mathrm{f}}{\mathrm{d}x} - gSJ \end{pmatrix}$$

Remarks:

- The terms $F(x,W)$ and $G(x,W)$ depend on x and W.
- To get a well-defined problem, it is necessary to add initial and boundary conditions.

If the hydraulic section S is strictly positive, the system of equations defined by Equation (6) is strictly hyperbolic. The Jacobian matrix reads:

$$DF(W,x) = \begin{pmatrix} 0 & 1 \\ \dfrac{-Q^2}{S^2} + \left(\dfrac{\partial P(x,S)}{\partial S}\right)_x & 2\dfrac{Q}{S} \end{pmatrix} \tag{7}$$

by setting

$$C = \sqrt{\left(\frac{\partial P}{\partial S}\right)_x}, \quad DF(W,x) = \begin{pmatrix} 0 & 1 \\ c^2 - u^2 & 2u \end{pmatrix}$$

The eigenvalues are: $\lambda_1 = u + c$, $\lambda_2 = u - c$ and associated eigenvectors:

$$r_1 = \begin{pmatrix} 1 \\ u + c \end{pmatrix}, \quad r_2 = \begin{pmatrix} 1 \\ u - c \end{pmatrix}$$

3. THE NUMERICAL SCHEME

In the first section, we present the numerical scheme for the homogeneous problem. The second section is devoted to the numerical treatment of the source terms.

3.1. Notations and definitions

The 1D domain Ω is divided into N cells $C_i = [x_{i-1/2}, x_{i+1/2}]$. The centre of C_i is called x_i.

The first and last cells are both half cells.

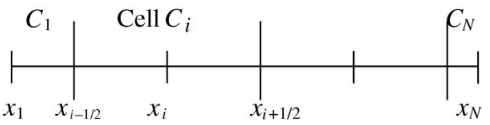

The time t belongs to the interval $[0,T]$ and the time step is denoted by Δt.

3.2. *Finite volume discretisation for the homogeneous problem*

The problem to be solved reads:

$$\begin{cases} x \in \Omega, \ \ t \in [0,T], \quad \Gamma \text{ is the boundary of } \Omega \\ \dfrac{\partial W(x,t)}{\partial t} + \operatorname{div} F(W,x) = 0 \\ W(x,0) = W_0(x) \\ \text{boundary conditions on } \Gamma \end{cases} \tag{8}$$

After integration of Equation (8) on $C_i x[t_n, t_{n+1}]$, for $i \in [1,M]$, we obtain:

$$\int_{C_i} (W(x,t_{n+1}) - W(x,t_n))\,\mathrm{d}x + \int_{t_n}^{t_{n+1}} (F(x_{i+1/2}, W(x_{i+1/2},t)) - F(x_{i-1/2}, W(x_{i-1/2},t))\,\mathrm{d}t = 0 \tag{9}$$

Therefore, the finite volume scheme is defined by:

$$\begin{aligned} W_{i,h}^{n+1} &= W_{i,h}^n - \frac{\Delta t}{\text{area}(C_i)}(F_{i+1/2}^n - F_{i-1/2}^n) = 0 \\ W_{i,h}^{n+1} &= \int_{C_i} W(x,t_{n+1})\,\mathrm{d}x, \quad W_{i,h}^n = \int_{C_i} W(x,t_n)\,\mathrm{d}x \end{aligned} \tag{10}$$

where

$$F_{i+1/2}^n = \int_{t_n}^{t_{n+1}} F(x_{i+1/2}, W(x_{i+1/2},t))\,\mathrm{d}t \text{ is the numerical flux}$$

Remark:

- $W_{i,h}^n$ is an approximation of the mean value of the exact solution on the cell C_i at the time step t_n.

The flux term $F_{i+1/2}^n$ is evaluated with a three-point scheme:

$$F_{i+1/2}^n = \phi(W_i^n, W_{i+1}^n)$$

The choice of the function ϕ is the key point for the whole definition of the scheme. Most of finite volume schemes developed to solve the shallow-water equations are based on Roe scheme [1–3, 5–7] which is robust, easy to implement and widely used.

Accordingly, we retain the Roe scheme to define this function. It consists of:
$\phi(W_i^n, W_{i+1}^n) = F(U_{ex}(0, W_i, W_{i+1}))$ where $U_{ex}(\xi, U_g, U_d)$ is the exact solution of a linearised Riemann problem:

$$\begin{cases} \dfrac{\partial U}{\partial t} + \tilde{A}(W_g, W_d)\dfrac{\partial U}{\partial x} = 0 \\ U(x,0) = \begin{cases} U_g \ si \ x < 0 \\ U_d \ si \ x > 0 \end{cases} \end{cases} \tag{11}$$

The matrix $\tilde{A} : \mathscr{R}^2 \times \mathscr{R}^2 \to M_2(\mathscr{R})$ must satisfy the following conditions:

1. $\tilde{A}$ continuous,
2. $\tilde{A}(U_g, U_d)(U_g - U_d) = F(U_g) - F(U_d)$;
3. $\tilde{A}(U_g, U_d)$ diagonalisable with real eigenvalues.

The two first conditions imply that $\tilde{A}(U, U) = DF(U)$ (consistancy).

Under these previous assumptions, the numerical flux $\phi(U_g, U_d)$ can be rewritten as:

$$\phi(U_g, U_d) = F(U_g) + \tilde{A}^-(U_g, U_d)(U_d - U_g) \tag{12}$$

$$\phi(U_g, U_d) = F(U_d) + \tilde{A}^+(U_g, U_d)(U_d - U_g) \tag{13}$$

$$\phi(U_g, U_d) = \frac{F(U_g) + F(U_d)}{2} - \tfrac{1}{2}|\tilde{A}(U_g, U_d)|(U_d - U_g) \tag{14}$$

Remarks:

- The time step for this scheme is classically limited by a Courant Friedrich–Levy condition.
- This scheme is a first-order scheme in space and time.

Now, we are going to define the Roe matrix. The main difficulties with the Roe scheme are:

1. To find a matrix that satisfies the assumption 2. If it is not possible, this can be overcome by using a method developed by Buffard *et al.* [15] and Eymard *et al.* [16]. Within this scheme, it is possible to avoid building the Roe matrix.
2. The Roe scheme does not fulfil the entropy condition which ensures the convergence towards a physical solution of the problem.

3.2.1. Construction of the Roe matrix. To determine the Roe matrix, we use a method developed by Roe [17, 18] for the Euler equations.

This method is based on the use of a parameter vector chosen in such a manner that U and $F(U)$ are homogeneous functions of degree 2 of W. By comparison with the Euler equations, the parameter vector is equal to:

$$W = \begin{pmatrix} \sqrt{S} \\ u\sqrt{S} \end{pmatrix}$$

Therefore, the Roe matrix is defined by:

$$\tilde{A}(W_g, W_d) = \begin{pmatrix} 0 & 1 \\ \tilde{c} - \tilde{u}^2 & 2\tilde{u} \end{pmatrix} \quad \text{with} \quad \tilde{u} = \frac{u_g\sqrt{S_g} + u_d\sqrt{S_d}}{\sqrt{S_g} + \sqrt{S_g}}$$

and

$$\tilde{c} = \frac{P(S_g, x) - P(S_d, x)}{S_g - S_d}$$

The eigenvalues of the Roe matrix are:

$$\tilde{\lambda}_1 = \tilde{u} + \tilde{c}, \quad \tilde{\lambda}_2 = \tilde{u} - \tilde{c}$$

We can associate the following eigenvectors:

$$\tilde{r}_1 = \begin{pmatrix} 1 \\ \tilde{u} + \tilde{c} \end{pmatrix} \quad \tilde{r}_2 = \begin{pmatrix} 1 \\ \tilde{u} - \tilde{c} \end{pmatrix}$$

If $W_g = \alpha_{1,g}\tilde{r}_1 + \alpha_{2,g}\tilde{r}_2$ and $W_d = \alpha_{1,d}\tilde{r}_1 + \alpha_{2,d}\tilde{r}_2$, the flux is totally defined by:

$$\phi(W_g, W_d) = \frac{F(U_g) + F(U_d)}{2} - \tfrac{1}{2}(|\tilde{u} + \tilde{c}|(\alpha_{d,1} - \alpha_{g,1})\tilde{r}_1) + (|\tilde{u} - \tilde{c}|(\alpha_{d,2} - \alpha_{g,2})\tilde{r}_2) \tag{15}$$

3.2.2. The entropy correction. One of the main drawbacks of the Roe solver is that it does not satisfy the entropy condition. It can allow non-entropic stationary discontinuity near the sonic points. To avoid this problem, it is necessary to modify the flux computation near the points where an eigenvalue $\lambda_{m=1,2}(\tilde{W})$ is close to zero.

Several possibilities are available. We have chosen the entropic correction defined by Leveque [19].

$$\lambda_m(\tilde{W}) \text{ is modified by } \lambda_m(W_d)\left(\frac{\lambda_m(\tilde{W}) - \lambda_m(W_g)}{\lambda_m(W_d) - \lambda_m(W_g)}\right)$$

3.3. Source terms

Source terms play an important role in the shallow-water equations. Their numerical treatment necessitates much care in order to avoid a dramatic loss of accuracy; for instance, flat water initially at rest starts moving artificially. It might also prevent the convergence to a real steady state at constant discharge.

The 1D shallow-water equations admit two main kinds of source terms:

- Source term linked to the geometry. This term is due to the bottom gradient and to the variation of the river width and comes from the splitting of the term $gS((\partial Z)/(\partial x))$. It reads:
$$\left(\frac{\partial P(x,S)}{\partial x}\right)_{z=\text{cte}} = \left(\frac{\partial P(x,S)}{\partial x}\right)_{S=\text{cte}} + \frac{\partial P(x,S)}{\partial S}\left(\frac{\partial S}{\partial x}\right)_{z=\text{cte}}$$
- The friction term: $-gSJ$ where $J = (Q^2)/(K^2S^2R_h^{4/3})$

The discretization is an essential and difficult step of the numerical scheme which finally must satisfy the following:

- Water at rest must stay at rest (no perturbation on the discharge).
- Good convergence towards a steady state (constant discharge free of oscillations).

Two paths can be followed in order to approximate the source terms $\iint_{c_i x \Delta t} B(x, W^n)\,\mathrm{d}x\,\mathrm{d}t$:

- A point-wise approximation leads to approximate the previous term by: $C_i \Delta t B(x_i, W_i^n)$. This simple method does not allow the two first criteria to be met because the discretization of the source term is not compatible with the upwind discretization of the pressure term.
- An upwind approximation similar to that used for the pressure term on the LHS.

In the literature, few papers concern the upwinding of the source terms. This problem has been tackled by Vasquez-Cendon [20] for the 2D shallow-water equations and for the 1D shallow-water equations with a locally rectangular channel [21] and an approximated conservation property has been established (the idea is equivalent to the notion of 'well balanced scheme' developed by Greenberg and Leroux [10]). Thus, we have adapted this method for the 1D shallow-water equations for an actual river without any assumption on the form of the section. We shall demonstrate that in case of an actual river, a mixed discretization (upwinded and centred) of the source term must be applied to obtain the approximated conservation property.

3.3.1. The upwinding of the source terms. We recall the upwinded technique developed by Vasquez-Cendon. More details are given in Reference [20].

To find the upwind flux, the source terms are projected on the eigenvectors basis $\tilde{X}(W)$ of the Roe matrix.

We denote:

- $\beta(W,x)$ the components of the source term $G(x,W)$ in this basis.
- $\tilde{\Lambda}$ the diagonal matrix of the eigenvalues of $\tilde{A} = X(\tilde{W})\tilde{\Lambda}X^{-1}(\tilde{W})$.
- $\tilde{\Lambda}^+$ the diagonal matrix of the positive eigenvalues of $\tilde{A}$.
- $\tilde{\Lambda}^-$ the diagonal matrix of the negative eigenvalues of $\tilde{A}$.

$$G(x,W) = X(\tilde{W}) \cdot \beta(W,x) = X(\tilde{W}) \cdot (\tilde{\Lambda}\tilde{\Lambda}^{-1})\beta(W,x)$$

By using the relations between $\tilde{\Lambda}^+$, $\tilde{\Lambda}^-$ and $|\tilde{\Lambda}|$, we obtain:

$$\begin{aligned} G(x,W) &= X(\tilde{W}) \cdot \tilde{\Lambda}^+\tilde{\Lambda}^{-1} \cdot \beta(W,x) + X(\tilde{W}) \cdot \tilde{\Lambda}^-\tilde{\Lambda}^{-1}\beta(x,W) \\ &= X(\tilde{W}) \cdot \left[\frac{1}{2}(I + |\tilde{\Lambda}|\tilde{\Lambda}^{-1})\right] X(\tilde{W}) \cdot G(X,W) \\ &\quad + X(\tilde{W}) \cdot \left[\frac{1}{2}(I - |\tilde{\Lambda}|\tilde{\Lambda}^{-1})\right] X(\tilde{W}) \cdot G(X,W) \end{aligned} \tag{16}$$

By analogy with the numerical treatment of the flux in the LHS, we define two flux functions Ψ_l and Ψ_r

$$\Psi_l = 2X(\tilde{W}) \cdot \left[\frac{1}{2}(I + |\tilde{\Lambda}|\tilde{\Lambda}^{-1})\right] X(\tilde{W}) \cdot G(X, W) \tag{17}$$

$$\Psi_r = 2X(\tilde{W}) \cdot \left[\frac{1}{2}(I - |\tilde{\Lambda}|\tilde{\Lambda}^{-1})\right] X(\tilde{W}) \cdot G(X, W) \tag{18}$$

The contribution of the source terms is evaluated in each cell i by:

- a part from the right interface $\int_{x_i}^{x_{i+1/2}} \Psi_r \, dx$
- a part from the left interface $\int_{x_{i-1/2}}^{x_i} \Psi_l \, dx$

3.3.2. Mixed discretization of the source terms. In the previous section, three different source terms have been defined because it allows them to be discretized in separate ways:

(1) $S_1 = \left(\dfrac{\partial P(x,S)}{\partial x}\right)_{S=\text{cte}}$

(2) $S_2 = \dfrac{\partial P(x,S)}{\partial S}\left(\dfrac{\partial S}{\partial x}\right)_{z=\text{cte}}$

(3) $S_3 = \dfrac{Q^2}{K^2 S^2 R_h^{4/3}}$

Term (1) is approximated by a centred discretization. The contribution on cell i is:

$$\int_{x_{i-1/2}}^{x_{i+1/2}} S_1(x_i, W_i) \, dx$$

Terms (2) and (3) are upwinded following the previous technique. Therefore the contribution on cell i of the source S_2 and S_3 is:

$$\int_{x_i}^{x_{i+1/2}} \Psi_r \, dx + \int_{x_{i-1/2}}^{x_i} \Psi_l \, dx \text{ with}$$

$$\Psi_r = 2X(\tilde{W}) \cdot \left[\frac{1}{2}(I - |\tilde{\Lambda}|\tilde{\Lambda}^{-1})\right] X(\tilde{W}) \cdot (G_2(x_{i+1/2}, W_i, W_{i+1}) + G_3(x_{i+1/2}, W_i, W_{i+1}))$$

$$\Psi_l = 2X(\tilde{W}) \cdot \left[\frac{1}{2}(I + |\tilde{\Lambda}|\tilde{\Lambda}^{-1})\right] X(\tilde{W}) \cdot (G_2(x_{i-1/2}, W_i, W_{i-1}) + G_3(x_{i+1/2}, W_i, W_{i-1}))$$

with $G_2 = (0, S_2)$ and $G_3 = (0, S_3)$

Conservation property. With this approximation, it is possible to demonstrate that a conservation property is satisfied.

By application of the Roe Solver on the homogeneous system, we obtain:

For cell i:

$$\Phi(W_i, W_{i+1}) = \begin{pmatrix} -\dfrac{\tilde{c}_{i+1/2}}{2}(S_{i+1} - S_i) \\ (P_{i+1/2}(S_{i+1}) + P_{i+1/2}(S_i))/2 \end{pmatrix}$$

$$\Phi(W_{i-1}, W_i) = \begin{pmatrix} -\dfrac{\tilde{c}_{i-1/2}}{2}(S_i - S_{i-1}) \\ (P_{i-1/2}(S_i) + P_{i-1/2}(S_{i-1}))/2 \end{pmatrix}$$

Computation of source terms. In case of initial state of rest, the source terms are directly linked to the variation of geometry.

On cell i, there are three contributions:

1. S_2 at the interface $i - 1/2$,

$$\Delta t \begin{pmatrix} -\dfrac{1}{2\tilde{c}_{i-1/2}}(P_{i-1/2}(S_i) - P_{i-1/2}(S_{i-1})) \\ (P_{i-1/2}(S_i) - P_{i-1/2}(S_{i-1}))/2 \end{pmatrix}$$

2. S_1 in the centre of cell i,

$$\Delta t \begin{pmatrix} 0 \\ (P_{i+1/2}(S_i) - P_{i-1/2}(S_i)) \end{pmatrix}$$

3. S_2 at the interface $i + 1/2$

$$\Delta t \begin{pmatrix} -\dfrac{1}{2\tilde{c}_{i+1/2}}(P_{i+1/2}(S_{i+1}) - P_{i+1/2}(S_i)) \\ (P_{i+1/2}(S_{i+1}) - P_{i+1/2}(S_i))/2 \end{pmatrix}$$

By writing the flux balance on cell i together with the computation of the source terms, one obtains easily: $W_i^{n+1} = W_i^n$

4. NUMERICAL RESULTS

The numerical results presented here have been obtained with the MASCARET code designed at EDF—LNH (Electricité de France—Laboratoire National d'Hydraulique) where the numerical scheme previously presented is implemented. The results are organized in three parts.

In the first part, we consider analytical problems for which an exact solution can be computed. In the second part, we present numerical results on a test-case which models a typical singularity of a valley. The numerical results are compared with measurements on physical models.

All the previous test-cases (analytical and experimental) have been defined for a working group initiated by EDF—LNH in the framework of IAHR [22,23]. This working group has gone on in a Concerted Action on Dam Break Model (CADAM), the aim of which is the validation of software dedicated to dam-break wave simulation.

Finally, in the third part, a real-life application is presented for a dam-break wave simulation.

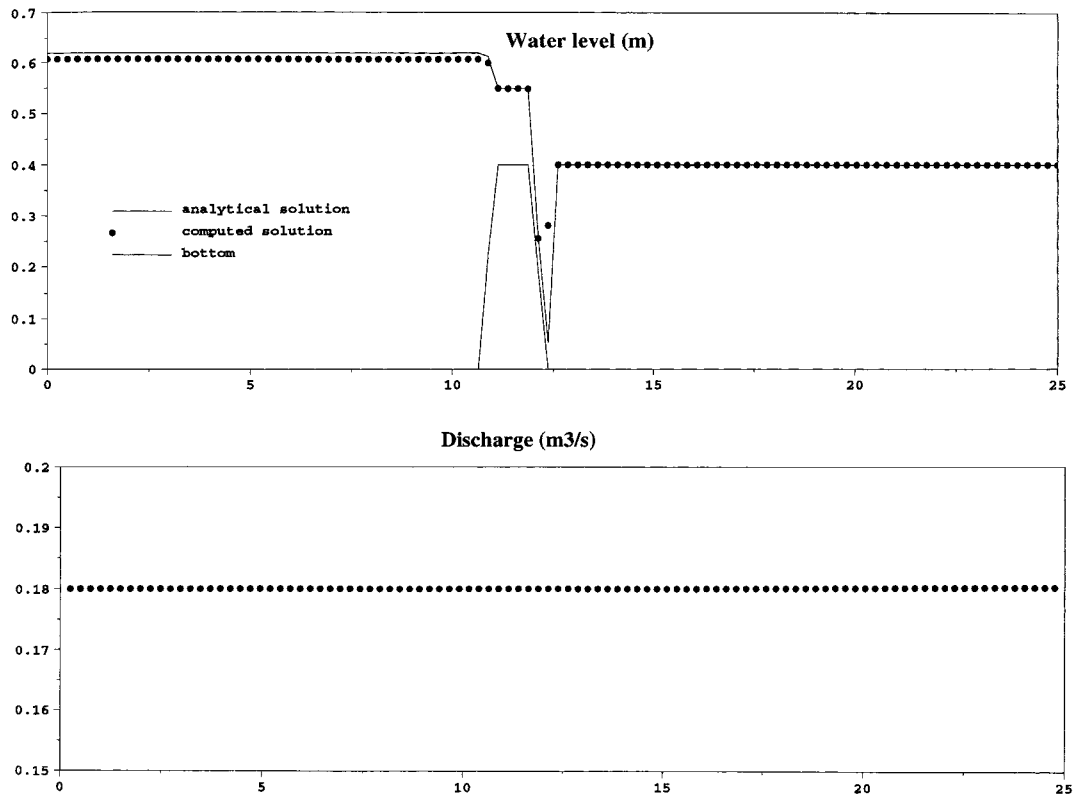

Figure 2. Flow over a bump in the case of transcritical flow with a shock.

4.1. Analytical test-cases

The analytical test-cases are split into two parts:

1. Steady flow
   - Flow at rest in a rectangular channel with a variable width, variable bottom and without friction.
   - Flow over a bump. According to the boundary conditions, the flow can be transcritical with or without shocks, subcritical and supercritical.
2. Unsteady flow
   - Dam-break on a dry bottom in a horizontal rectangular channel with a constant width and without friction (Ritter analytical solution).

The simulation of flow at rest and flow over a bump enables one to check that the source terms are correctly evaluated. In the case of a flow at rest, the upwinding of the source terms, as we describe later, allows one to obtain a computed discharge both constant and zero valued.

Since the test of a flow over a bump is more interesting than a flow at rest, we present the results of the test of a flow over a weir. The crest of the weir is equal to 0.4 m. For this

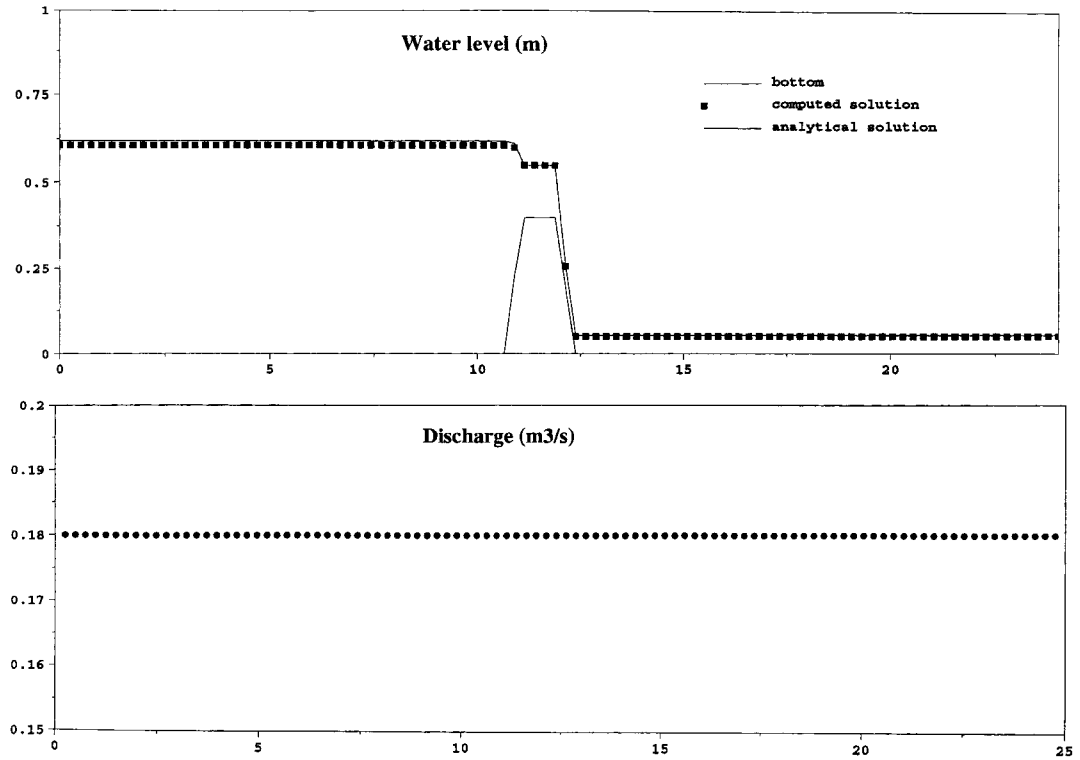

Figure 3. Flow over a bump in the case of transcritical flow.

case, the initial state is a constant water level equal to 0.4 m. At the inlet of the domain, the discharge is imposed equal to $0.18\,m^3\,s^{-1}$ and at the outlet, the water level is fixed equal to 0.4 m. Figure 2 shows the steady flow obtained in the case of the above-mentioned boundary conditions. These results have been obtained with a constant mesh equal to 0.25 m. Therefore, we can note that the weir is described with only four points (the slope of the weir is equal 0.4/0.25). The time step is fixed in respect of the CFL condition. It is worth noting that the discharge (mass fluxes) is constant without any perturbation. Moreover, despite the steep slope of the weir, the shock is quite well computed.

In order to check that the downstream boundary condition does not alter the water level upstream the weir, a simulation has been performed by decreasing the fixed water level downstream; the flow becomes transcritical without shocks. In Figure 3, the computed results are compared against the analytical solution and we note the right behaviour and the satisfying accuracy of the computed flow.

The unsteady flow test-cases have been chosen because they include some of the difficulties of an actual dam-break wave simulation; for instance, propagation over a dry bottom and discontinuous initial water level. The initial problem is a Riemann problem:

- if $x > 0$, the water level and the discharge are equal to zero
- if $x < 0$, the water level is equal to 6 m and the discharge is equal to zero.

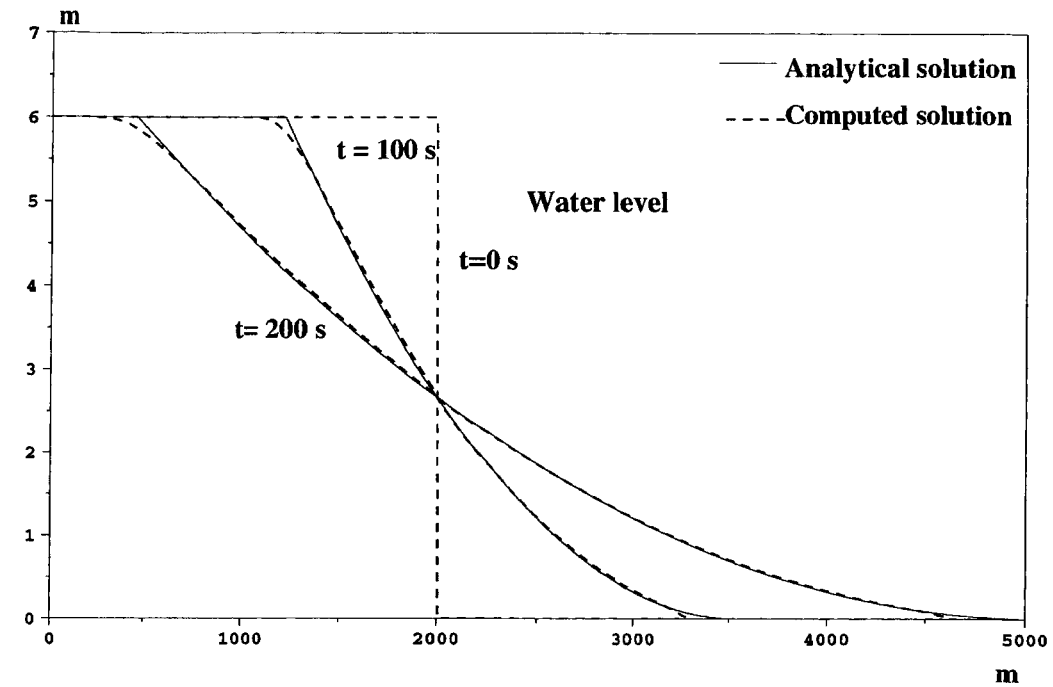

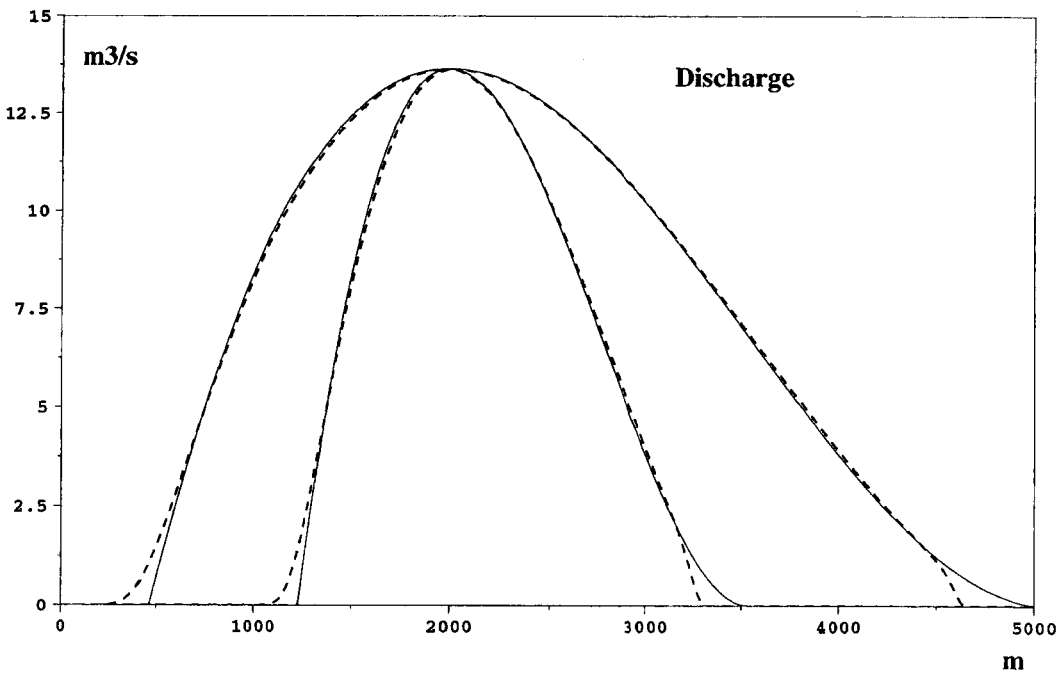

Figure 4. The Ritter test-case. Comparison between analytical solution and computed solution.

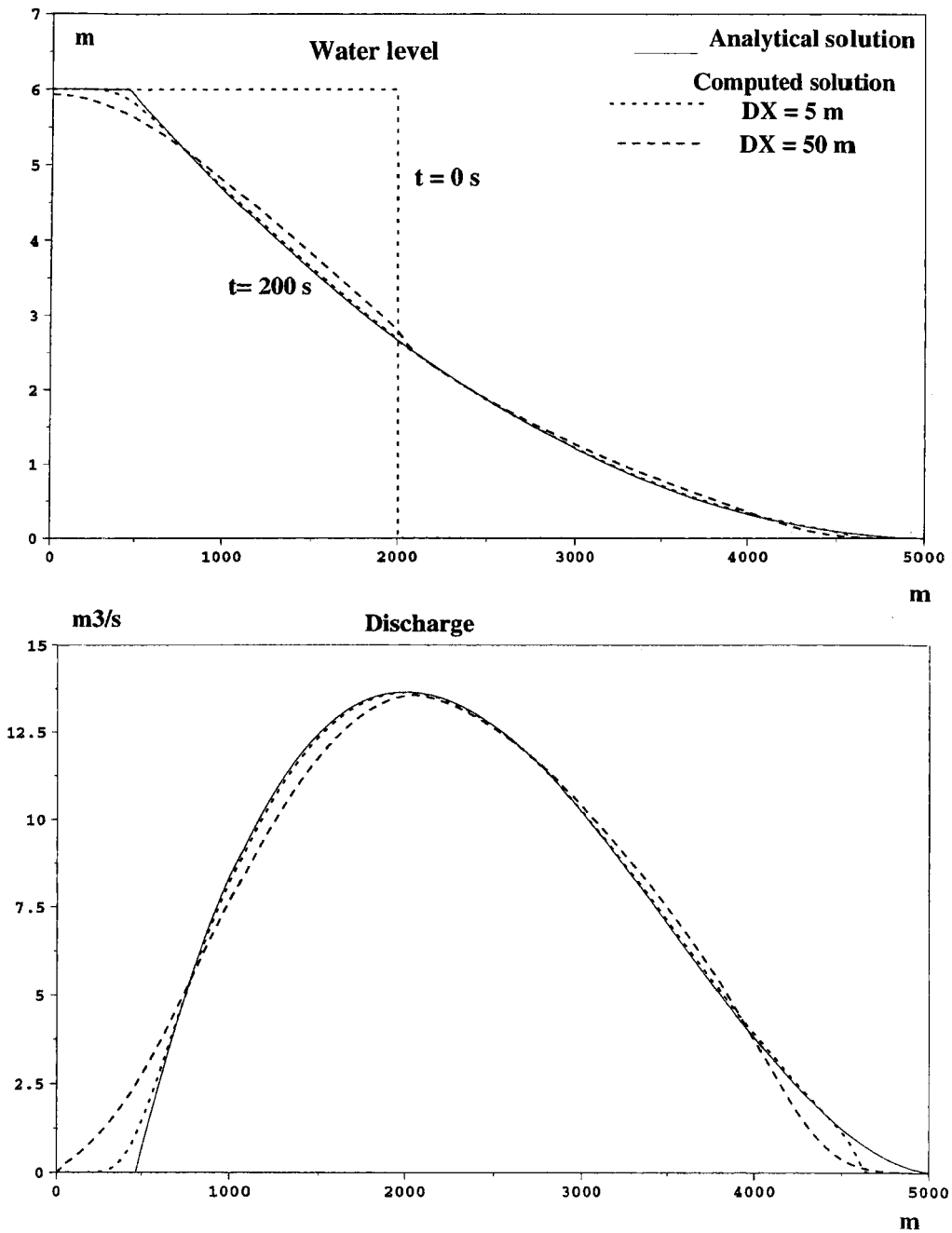

Figure 5. Influence of the mesh size.

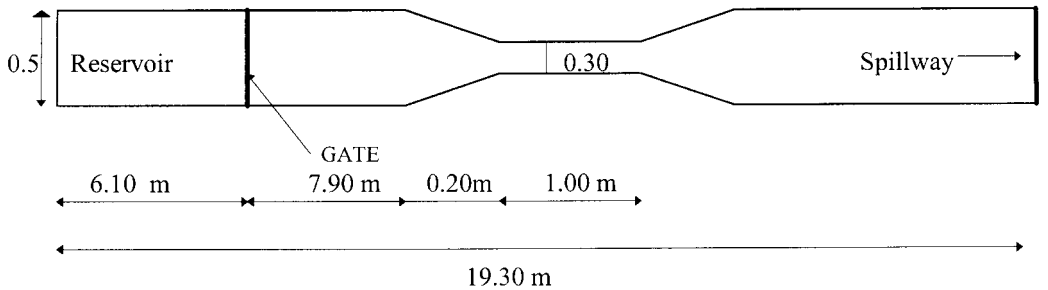

Figure 6. Geometry of the physical model.

The analytical solution includes a rarefaction wave that propagates upstream the initial discontinuity and a bore that propagates downstream over dry bed. In Figure 4, the comparison between analytical and computed solutions is presented. We can note a good agreement between the two curves. These results have been obtained with a constant mesh size equal to 5 m and with a time step in respect of the CFL condition.

Figure 5 shows the influence of the mesh size on the solution. The accuracy is improved: less diffusion for the rarefaction wave and better approximation of the bore velocity.

4.2. Experimental test-cases

In the framework of an IAHR working group, the experimental test-cases have been achieved by the IST (Lisboa), the UCL (Bruxelles) and by the MET (Louvain-La-Neuve). Each test-case modelizes a typical singularity of a valley:

- Contraction of a channel to model a rock lock in a valley (IST).
- Sudden enlargement to model an outlet of the valley in a flood plain (IST and MET).
- A channel with a 90° bend to model a curve in a river (UCL).

We present the results of the MASCARET code only in the case of a channel with a constriction (see Figure 6) achieved by the IST ([23]).

The initial problem is a Riemann problem as in the Ritter test-case. The water level is equal to 0.3 m. The friction term corresponds to a Strickler coefficient of 80.

The numerical results are compared with the measurements at four gauges. Figure 7 shows the comparison.

The mesh size is constant, equal to 0.4 m, and the time step corresponds to a CFL of 0.8.

Gauge 1 shows the propagation of the rarefaction wave in the reservoir. This rarefaction wave is correctly approximated. On gauge 2, we remark on the propagation with a negative velocity of a jump due to the constriction. The approximated solution models this discontinuity well. Moreover, we can note that the time propagation (gauges 3 and 4) is well computed which is essential for dam-break wave simulation.

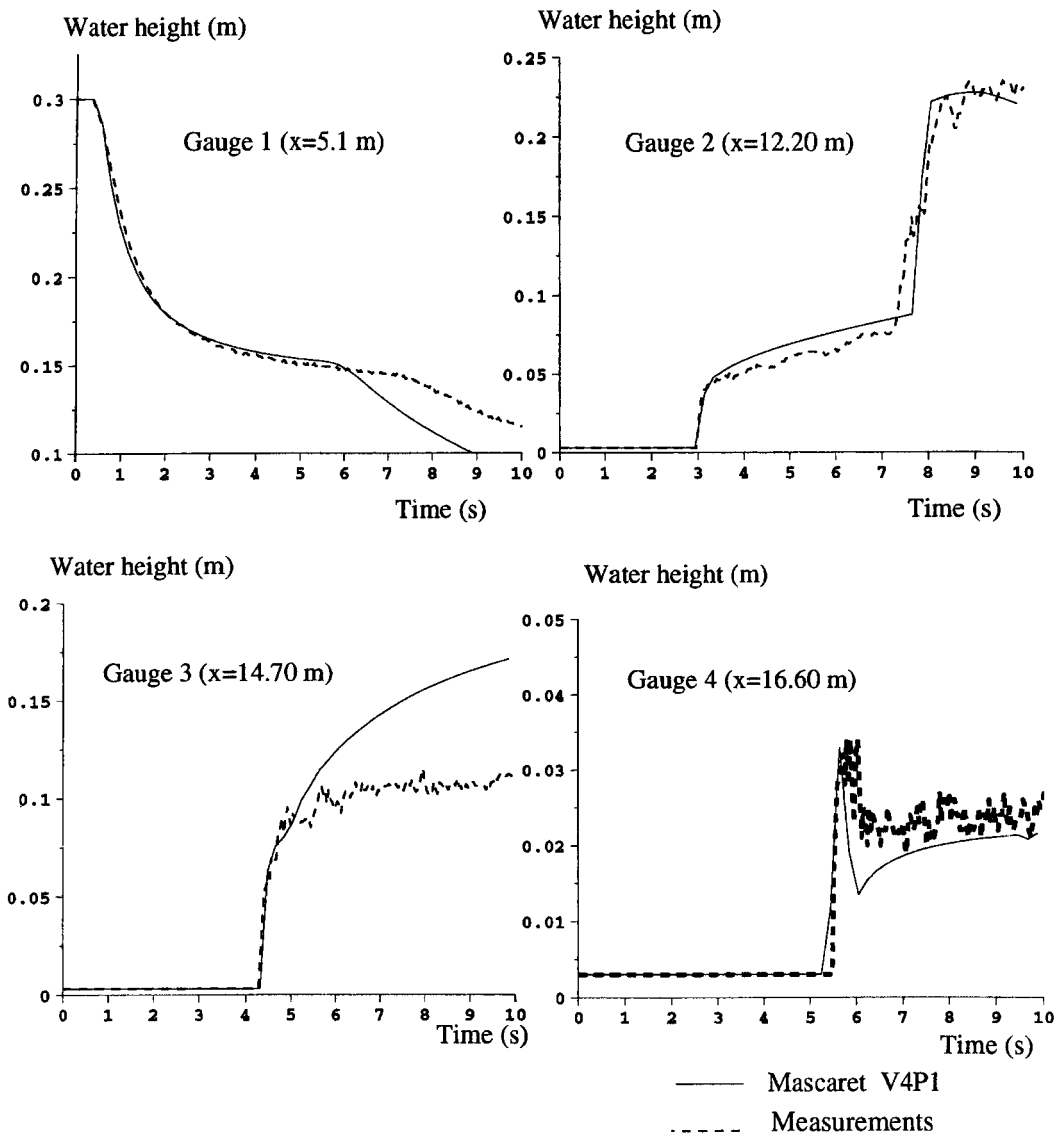

Figure 7. Comparison between the measurements and the approximated solution at the different gauges.

Four gauges are located in the middle of the channel to record the water level.

1. Gauge 1: 1.00 m upstream the dam.
2. Gauge 2: 6.10 m downstream the dam.
3. Gauge 3: 8.60 m downstream the dam.
4. Gauge 4: 10.50 m downstream the dam.

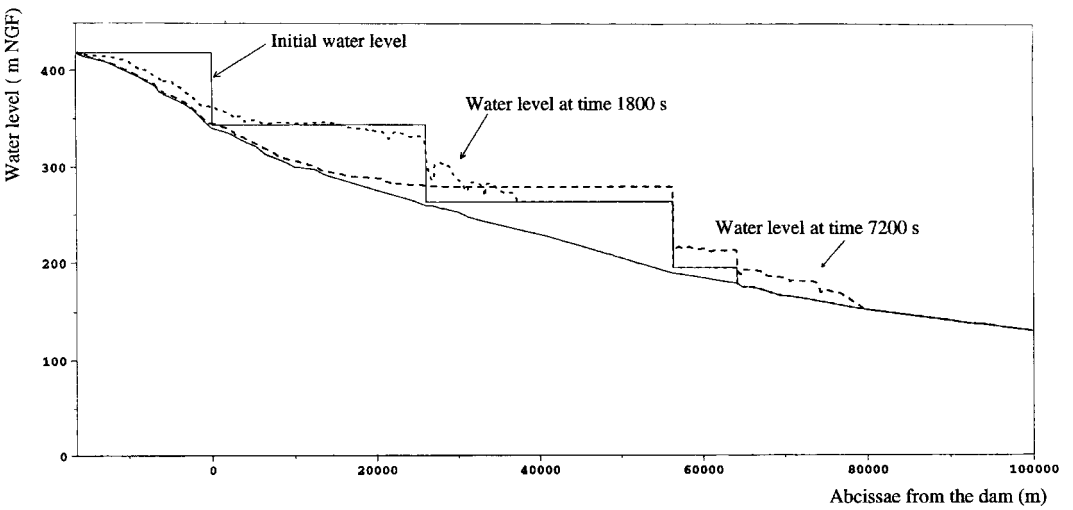

Figure 8. Water level at $t = 1800$ s and 7200 s.

4.3. *Real dam-break wave simulation*

The software described in the previous chapters has already been used to perform many studies. In order to illustrate the complexity of such simulations, we will show the results obtained on a dam-break simulation on an actual valley.

The features of this computation are:

- Main dam height = 80 m.
- Reservoir capacity = 4.8×10^8 M^3.
- Valley length = 150 km.
- Three dams downstream the main dam: two of them resist all along the simulation and the other collapses when the wave arrives.
- Initially, the valley downstream the main dam is dry except in the reservoirs.

In Figure 8, the water level at different time steps is presented. We can note that dams 1 and 4 have already collapsed and dams 2 and 3 resist the flow. The overtopping has been modelled as a flow over a weir.

In Figure 9, we remark on the important variations of the hydraulic section and of the Froude number which can reach a value as high as 4. It illustrates very well the features (large variations of hydraulic sections, very unsteady flow) of dam-break wave simulation in an actual valley.

5. CONCLUSION

Modelling free-surface flows for applications such as dam-break wave simulation, reservoir emptying and flooding leads to the solution of a non-linear hyperbolic system with a non-conservative term in the momentum equations. In order to be able to apply classical schemes developed for hyperbolic systems, this non-conservative term is split in two terms: one con-

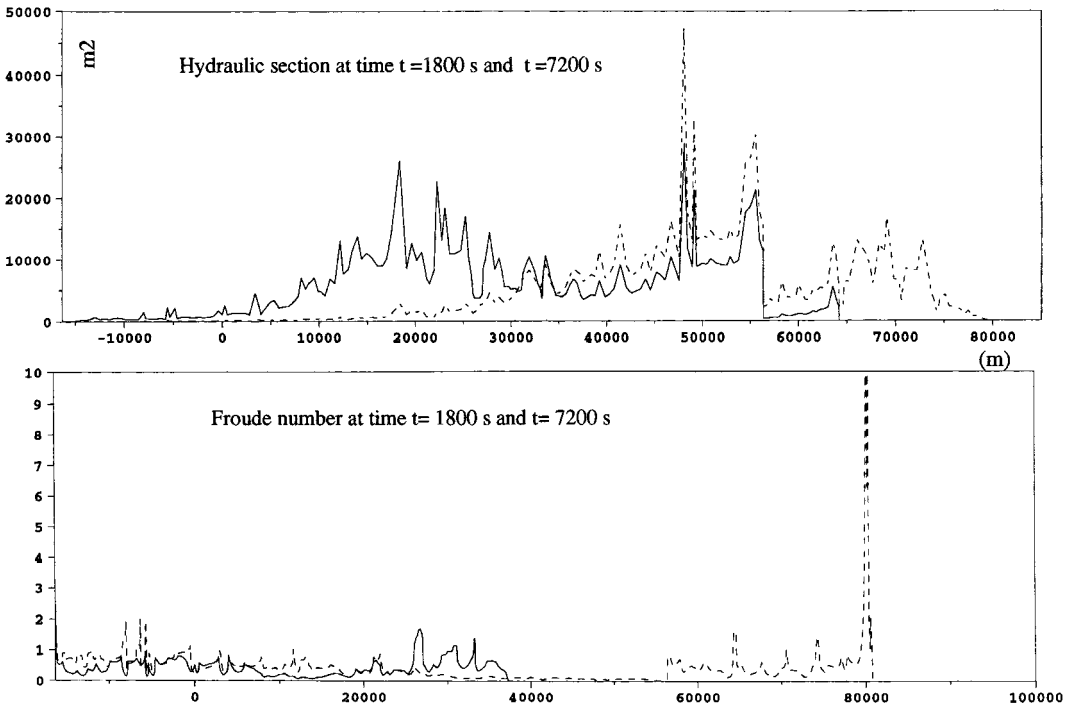

Figure 9. Hydraulic section and Froude number at $t = 1800$ s and 7200 s.

servative on the LHS and the other one on the RHS. The main drawback of this method is to have to deal with stiff source terms. One of the difficulties is to keep the equilibrium for a steady flow.

For the homogeneous problem, a Roe scheme is used. The source terms have been split in two parts to allow a separate discretization. An upwinding scheme developed by Vasquez-Cendon ([20]) has been applied to one of the two components, a centred discretization to the other one.

This scheme allows us to check the constraints imposed by the applications:

- To converge to a steady state without perturbation on the discharge.
- To propagate a bore over dry areas.
- To deal with the hydraulic jump.

Numerical solutions have been represented on analytical test-cases. The results show that:

- in case of steady state, the equilibrium is correctly approximated,
- the scheme is suitable for propagation over dry areas.

Moreover, comparisons with measures on physical models confirm the good behaviour of the numerical scheme in the case of dam-break wave simulation. Finally, simulation of an actual dam-break wave illustrates the robustness of the scheme and its ability to deal with the problem of a dam-break wave simulation.

REFERENCES

1. Braschi G, Dadone F, Gallati M. Plain flooding: near field and far field simulations. *Proceedings of the Specialty Conference*, *Modelling of Flood Propagation over Initially Dry Areas*, 1994.
2. Monthe LA. Etude des équations aux dérivées partielles hyperboliques raides. Application aux équations de Saint-Venant. Thesis, Université de Rouen, France, 1997.
3. Monthe LA, Benkaldoum F, Elmahi I. Positivity preserving finite volume Roe schemes for transport-diffusion equations. *Computer Methods in Applied Mechanics and Engineering* 1999; **15**:1–20.
4. Toro EF. *Riemann Solvers and Numerical Methods for Fluid Dynamics*. Springer-Verlag: Berlin, Heidelberg, 1997.
5. Naaim M, Brugnot G. Free surface flow modelling on a complex topography. *Proceedings of the Specialty Conference*, *Modelling of Flood Propagation over Initially Dry Areas*, 1994.
6. Paquier A. Modélisation et simulation de la propagation de l'onde de rupture de barrage. Thesis, Université Jean Monnet, Saint-Etienne, France, 1995.
7. Glaister P. Approximate Riemann solutions of the shallow-water water equations. *Journal of Hydraulic Research* 1988; **26**:293–306.
8. Buffard T. Analyse de quelques méthodes volumes finis non structurés pour la résolution des équations d'Euler. Thesis, Université de Paris VI, France, 1993.
9. Bon C. Modélisation et simulation numérique d'écoulements hydrauliques et de ruissellement en topographie quelconque. Thesis, Université de Bordeaux I, France, 1997.
10. Greenberg JM, Leroux AY. A well balanced scheme for the numerical processing of source terms in hyperbolic equations. *SIAM Journal on Numerical Analysis* 1996; **33**(1):1–16.
11. Herard JM. Solveur de Riemann approché pour un sysrème hyperbolique non conservatif issu de la turbulence compressible. *Rapport EDF HE-41/95/009/A*, Département LNH, 6, Quai Watier, Chatou, France.
12. Lecoz O. Un schéma équilibre pour les écoulements à surface libre instationnaires avec bathymétrie. Thesis, Université de Bordeaux, France, 1996.
13. Brun G, Herard JM, Jeandel D, Uhlmann M. An approximate Riemann solver for second moment closures. *Journal of Computational Physics* 1999; **151**(2):990–996.
14. Chinnayya A, Le Roux AY. *A new general Riemann solver for the shallow-water equations with friction and topography*, 1999. Available in the conservation law preprint server http://www.math.ntnu.no/conservation/.
15. Buffard T, Gallouet T, Herard JM. Un schéma simple pour les équations de Saint-Venant. *Comptes Rendus de l'Académie des Sciences* 1998; **I-326**:385–390.
16. Eymard R, Gallouet T, Herbin R. Finite volume methods. *Handbook for Numerical Analysis*. P.G. Ciarlet, P.L. Lions (eds), North-Holland, 1999.
17. Roe PL. Approximate Riemann solvers parameters vectors and difference schemes. *Journal of Computational Physics* 1981; **43**:357–372.
18. Roe PL. Some contributions to the modelling of the discontinuous flow. *Lecture in Applied Mathematics* 1985; **22**:163–193.
19. Leveque RJ. Numerical methods for conservation laws. *Lecture in mathematics ETH Zurich*. Birkhaüser: Basel/Boston/Berlin, 1990.
20. Vazquez-Cendon ME. Estudio de esquemeas descentrados para su application a las leys de conversacion hiperbolicas con terminos fuente. Thesis, Universidad Santiago de Compostela, Spain, Vazquez-Cendon 1994.
21. Vazquez-Cendon ME. Improved treatment of source terms in upwind schemes for the shallow-water equations in channels with irregular geometry. *Journal of Computational Physics* 1999; **148**:497–526.
22. *Working Group on Dam-Break Modelling*. Meeting report, Université Catholique de Louvain and Université Libre de Bruxelles, Belgique, 1997.
23. Goutal N, Maurel F. Proceedings of the 2nd workshop on dam-break wave simulation. *Technical report HE-43/97/016/A*, Département Laboratoire National d'Hydraulique, 6, Quai Watier, Chatou, France.

